Pump–probe spectroscopy of the hydrated electron: A quantum molecular dynamics simulation

Benjamin J. Schwartz and Peter J. Rossky
Department of Chemistry and Biochemistry, University of Texas at Austin, Austin, Texas 78712-1167

(Received 2 June 1994; accepted 1 July 1994)

Quantum nonadiabatic molecular dynamics simulations are used to directly compute the transient absorption spectroscopy following photoexcitation of equilibrium hydrated electrons. The calculated spectral transients are found to be in excellent agreement with ultrafast traces measured in recent transient spectral hole-burning experiments [Barbara and co-workers, J. Chem. Phys. **98**, 5996 (1993); J. Phys. Chem. **98**, 3450 (1994)], indicating that the computer model correctly captures the underlying physics. The model transients are dissected into ground state bleach, excited state absorption, and stimulated emission spectral components, each of which is examined individually and analyzed in terms of the microscopic solvent response following photoexcitation. Although there is no distinct spectral hole, bleaching dynamics are found to play an important role in the overall transient spectroscopy. The excited state absorption spectrum undergoes a complex evolution due to solvation dynamics which alters both the frequencies and the oscillator strengths of the relevant quantum transitions. Calculated excited state emission from the electron is characterized by an enormous dynamic Stokes shift as well as an overall spectral narrowing in time. In combination, these three components allow the assignment of features of the measured ultrafast spectroscopic transients in terms of specific details of the microscopic solvent response.

I. INTRODUCTION

The study of excess electrons in liquids provides the simplest context for investigation of the coupling between the electronic states of solutes and solvent fluctuations. The aqueous solvated electron in particular plays a central role in solution photochemistry and photoelectrochemistry and is a ubiquitous transient species in irradiated aqueous systems. Since the details of the underlying solute–solvent coupling are directly reflected in the electronic absorption spectrum, it is of little surprise that the transient spectroscopy of the hydrated electron has been the recent subject of intense experimental[1–5] and theoretical[6–11] interest.

There have been two different approaches exploring the ultrafast spectroscopy of the hydrated electron. The first experiments[1,2] studied the formation of the well-known equilibrium absorption spectrum following electron photoinjection into pure liquid water. An initial infrared absorption, assigned to an excited state of the hydrated electron, decayed smoothly into the known equilibrium absorption spectrum on a subpicosecond time scale. The measured transient spectroscopy can be understood via a predominantly two-state kinetic model[12,13] based on the behavior of detailed nonadiabatic computer simulations.[7,8] Overall, these experiments point out the importance of spectroscopic contributions from the excited state of the hydrated electron, as well as the extremely rapid equilibration of the ground state electron upon non-adiabatic transition.

In the second approach, Barbara and co-workers have examined the ultrafast spectroscopy following photoexcitation of equilibrium hydrated electrons.[3–5] In these experiments, an excitation pulse which is spectrally narrow compared to the absorption band of the hydrated electron is used to excite the subset of electrons which are in configurations that bring them into resonance with the pulse. Once this subset is promoted to the excited state, an absorption deficit, or spectral hole, is left at the frequency of the excitation pulse. As time progresses, solvent fluctuations randomize this subset of configurations and the hole broadens, leading eventually to a uniform bleaching of the entire absorption band. The promoted electrons can also transiently absorb to higher lying excited states, or undergo stimulated emission back to the ground state. Thus, the signal detected in these experiments, the difference in optical density from the equilibrium absorption of the hydrated electron at various time delays after excitation, contains contributions from ground state bleaching dynamics, excited state absorption evolution, and the dynamic Stokes shift of the stimulated emission.

The spectral transients measured in these photoexcitation experiments showed a complex mixture of absorption and bleaching dynamics, and could not be adequately described with a simple two-state picture.[4,10] Based on the results of the photoinjection experiments which indicated a very short excited state lifetime for the hydrated electron, an extension of the two-state kinetic model which incorporated, in addition, the effects of cooling in the ground state after the nonadiabatic transition was proposed to explain the data.[4] In an earlier publication,[10] we presented the essential spectral results of quantum molecular dynamics simulations modeling these experiments. The calculated spectral transients were in excellent agreement with experiment, indicating the simulations correctly capture the essential physics of the hydrated electron. The simulations, however, manifest a lifetime of the excited state after photoexcitation that was much longer than that found after injection. In combination with artificial spectral transients constructed by removing various absorption and bleaching components, this long lifetime suggested that ground state cooling is of little importance to the observed spectroscopy. Instead, the spectral complexity was assigned

 0021-9606/94/101(8)/6917/10/$6.00

to a combination of excited state solvation and ground state bleaching dynamics.[10]

In the preceding paper,[11] we have investigated the microscopic details of aqueous solvation dynamics following photoexcitation of the hydrated electron by computer simulation. The purpose of the present paper is to analyze in detail the manifestations of this molecular response in the ultrafast transient spectroscopy.

In order to pursue this, we first summarize the essential physical features of the system.[11] At equilibrium, the hydrated electron is characterized by a roughly spherical cavity which supports an *s*-like ground state, three *p*-like excited states which are split by 0.8 eV due to local asymmetry, and higher lying delocalized states comprising the conduction band of water.[6] Upon photoexcitation, the solvent undergoes rapid translational and reorientational motion to solvate the excited electron, forming a peanut-shaped cavity: water molecules diffuse into the nodal region of the *p*-like charge distribution, and rotate to accommodate the change from spherical to cylindrical symmetry. As solvation proceeds, the electron grows in size by a factor of ~2 along the axial direction of the lobes of the excited state wave function. All these changes have a pronounced effect on the eigenstates of the hydrated electron. The formerly *s*-like ground state must significantly distort to fill the peanut-shaped cavity, so its energy increases as solvation proceeds. Solvent molecules in the nodal plane of the occupied state interfere with the lobes of the upper two *p*-like states whose electron densities are oriented in this plane, raising the energy of these states, while the occupied *p*-like state undergoes little net change in energy.

The dynamics of this solvent response to photoexcitation of the hydrated electron is characterized by a 25 fs Gaussian inertial component (40%) and a 250 fs exponential decay (60%).[11] The ground state-excited state energy gap relaxes on these time scales (dynamic Stokes shift), while the gap between the occupied state and the higher lying *p*-like states undergoes an increase with similar dynamics. Despite the strong coupling of aqueous solvent fluctuations to the energy levels of the hydrated electron manifest in the enormous fractional Stokes shift (~75%), the solvation dynamics follows linear response. With the limitations of a ~300 fs instrument function,[4] the ~25 fs inertial contribution to the solvation response should not produce a strong spectroscopic signature, but the subsequent evolution of the quantum energy levels should be directly reflected in the ultrafast transient spectroscopy. The excited state absorption and emission spectra must evolve significantly due to the solvation response following excitation, and the ground state bleach samples the fluctuations broadening the equilibrium absorption spectrum. Thus, solvation dynamics must affect all the components comprising the observed optical signal in the photoexcitation experiments.

In this paper, we examine in detail the ultrafast transient spectroscopy of the hydrated electron calculated from quantum nonadiabatic molecular dynamics simulation. We compare the computed ultrafast spectral transients with experiment, and focus on the underlying reasons for the similarities and differences. The evolution of the individual ground state bleach, excited state absorption, and stimulated emission components comprising the observed spectroscopy is correlated with microscopic structural changes associated with the solvent response. Further, we present calculated spectroscopic traces for wavelengths not yet investigated by experiment. In particular, to the best of our knowledge, fluorescence has not yet been observed for photoexcited aqueous electrons in the laboratory; the analysis of the emission spectroscopy presented here provides incentive for future experimental studies along these lines.

II. METHODOLOGY

In this section, we describe the model system used to compute the ultrafast transient spectroscopy of the hydrated electron following promotion into the excited state, discuss the sampling of initial excited state configurations, and introduce formalism for the choice of an appropriate statistical weight.

A. Computational details

The nonadiabatic simulation procedures we employ are identical to those used in previous studies of electron localization after injection,[8] and have been described in both the preceding paper[11] and in the literature.[14,15] Briefly, the model system consisted of one quantum electron and 200 classical SPC flexible water molecules[16] in a cubic cell of side 18.17 Å (solvent density 0.997 g/ml) with standard periodic boundary conditions at room temperature. The electron–water interactions were described by a pseudopotential,[17] and the equations of motion integrated using the Verlet algorithm with a 1 fs time step. The adiabatic eigenstates at each time step were calculated via an efficient iterative and block Lanczos scheme[14] on a 16^3 grid; the lowest 6 eigenstates were computed during nonadiabatic dynamics, and the lowest 40 eigenstates were employed in all spectral computations.

Twenty configurations in which the electronic absorption of the hydrated electron was resonant with the pump laser (2.27 ± 0.01 eV corresponding[18] for the model Hamiltonian to a 780 nm experimental pump pulse with a bandwidth of ~200 cm^{-1}) were selected from a 35 ps equilibrated ground state trajectory[8] and used as the starting points for ground state bleach spectral computations. The transient bleach dynamics (spectral hole burning) $B(t;\omega)$ were computed as the spectrum the electron *would* have had by remaining on the ground state after these starting configurations (i.e., the removal of those configurations selected by the pump laser from the ensemble average comprising the equilibrium absorption spectrum).[19] Using the adiabatic eigenstates, the transition dipole matrix elements $\boldsymbol{\mu}_{fg}(t)=\langle\psi_f(t)|\mathbf{r}|\psi_g(t)\rangle$ between the final (f) and ground (g) states were computed every 3 time steps along the ground state trajectories, and the corresponding transient bleach spectra at time t after excitation computed directly as the sum over final states

$$B(t;\omega)\propto\sum_{f=2}^{40}|\boldsymbol{\mu}_{fg}(t)|^2\delta(\hbar\omega-E_f+E_g). \tag{1}$$

To improve statistical accuracy, the frequency dependence was computed by placing the squared transition dipoles into

0.1 eV bins corresponding to the ground state-final state energy difference, with each of the bins averaged independently.

Excited state absorption $A(t;\omega)$ and stimulated emission $S(t;\omega)$ contributions were computed from excited state trajectories initiated from these same 20 starting configurations. While the excited state (e) is the occupied state, the contribution of stimulated emission to the transient spectroscopy is given by the sum over all lower energy states:

$$S(t;\omega)\propto \sum_{\substack{i \\ (E_i<E_e)}} |\langle\psi_i(t)|\mathbf{r}|\psi_e(t)\rangle|^2\delta(\hbar\omega-E_e+E_i). \quad (2)$$

The contribution from absorption by the occupied state (initially the excited state and after radiationless transition the ground state) is determined from

$$A(t;\omega)\propto \sum_{\substack{i \\ (E_i>E_{\rm occ})}} |\langle\psi_i(t)|\mathbf{r}|\psi_{\rm occ}(t)\rangle|^2\delta(\hbar\omega-E_i+E_{\rm occ}). \quad (3)$$

Each of these is computed via the scheme described for the bleach.

Due to the short nonradiative lifetime of the excited hydrated electron, we have neglected the coupling to the vacuum which results in spontaneous fluorescence. Thus, the total *change* in absorption measured at time t (which is the optical signal measured experimentally) is given simply by the sum of these three contributions

$$\Delta OD(t;\omega)=A(t;\omega)-B(t;\omega)-S(t;\omega). \quad (4)$$

The computed instantaneous spectral dynamics were then convolved with a 300 fs Gaussian representing the experimental instrument function.[3,4] The issue of the role of this convolution in the correct statistical weights for different trajectories is discussed in the following section.

B. Statistics of photoexcitation of hydrated electrons

One of the key features of transient hole-burning spectroscopy is that the initial pump pulse selects only a specified subset of configurations for excitation. Since there are many ways in which configurations can be on resonance with the excitation laser (roughly 6% of all the configurations in the 35 ps ground state trajectory have an energy difference which falls within the laser bandwidth), it is important to determine the correct statistical weight for each starting configuration in the overall ensemble average. At the same time, it is important to avoid spending computational resources on trajectories with low statistical significance. In this section, we use perturbation theory and the correlation statistics of resonance times to derive an expression for weighting trajectories launched from different initial conditions. We will show that for the present system, it is acceptable to weight all resonant initial conditions in our sample equally.

The first question we address is simply the average time for resonance within the excitation bandwidth: given that a trajectory includes a resonant configuration, how long, on the average, does the trajectory stay on resonance? Figure 1 displays the joint probability $P(t)$ of a configuration being on resonance at time t given that its trajectory was also resonant at time zero. This probability decays rapidly, indicating that the fluctuating energy gap passes through the resonance window quite quickly, spending typically only one or two consecutive time steps within the laser bandwidth. For times $\geqslant$10 fs, this joint probability decays to ~6%, which is the simply the probability of finding a resonant configuration; in other words, there is no correlation between resonant configurations for times much longer than 10 fs. This observation, along with the rapid dephasing time calculated for electronic coherence between the ground and excited states of the hydrated electron,[20] indicates that for interaction with the radiation field, nonconsecutive series of resonant configurations can be treated as statistically independent events which should be given identical statistical weights. For the few cases where there are consecutive configurations on resonance, we turn to first-order time-dependent perturbation theory.

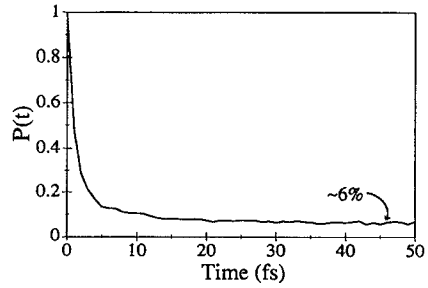

FIG. 1. Joint probability of finding a configuration on resonance given that it was also resonant at $t=0$. The asymptotic value of 6% represents the probability that any configuration meets the resonance condition.

For a quantum system interacting with an external field, the probability amplitude for finding the system in the final (f) excited state after interacting for time T is given by

$$a_f(T)=-\frac{i}{\hbar}\int_0^T dt\langle\psi_f|H_{\rm int}|\psi_g\rangle\exp\left(i\int_0^t dt'\ \omega_{fg}(t')\right). \quad (5)$$

Here, $\omega_{fg}(t)$ is the time-dependent energy gap between the ground and excited states, and $H_{\rm int}=-\boldsymbol{\mu}\cdot\mathbf{E}(t)\cos(\omega_L t)$ is the interaction Hamiltonian of the applied laser field with pulse envelope $E(t)$ and frequency ω_L. If we make the assumption of a square laser bandwidth (generalization to an arbitrary shape is straightforward) and also assume that the energy gap is equal to the central laser frequency ω_L for j consecutive resonant time steps, we obtain

$$a_f(j\Delta t)=\frac{i}{\hbar}\int_0^{j\Delta t} dt\langle\psi_f|\boldsymbol{\mu}|\psi_g\rangle\cdot\mathbf{E}(t)\cos(\omega_L t)e^{i\omega_L t}$$

$$=\frac{i}{2\hbar}\int_0^{j\Delta t} dt\ \boldsymbol{\mu}_{fg}\cdot\mathbf{E}(t)[e^{2i\omega_L t}+1], \quad (6)$$

where Δt is the time step. If we make the rotating wave approximation (neglecting the first term in the square brackets) and assume that $\mathbf{E}(t)\approx\mathbf{E}$ (which is rigorously true for a

square pulse of duration much longer than $j\Delta t$) during the time of interaction, then for a trajectory with j consecutive resonant configurations, we have

$$a_f(j\Delta t)\approx\frac{i}{2\hbar}j\Delta t\boldsymbol{\mu}_{fg}\cdot\mathbf{E}. \tag{7}$$

Since each *set* of consecutive configurations is taken to be statistically independent, the total probability Q for excitation from a trajectory with a *maximum* of M consecutive resonant configurations is given by

$$Q(M\Delta t)=Q_M=\sum_{m=1}^{M}\mathscr{P}_m|a_f(m\Delta t)|^2. \tag{8}$$

In Eq. (8), $\mathscr{P}_m$ is the probability of having m consecutive resonant configurations [$\mathscr{P}_m$ can be obtained as $\Pi_{n=1}^{m}P(n)$, where $P(n)$ is the joint probability distribution displayed in Fig. 1] and the sum accounts for all possible ways to launch the trajectory from any point in the consecutive sequence. For a square excitation pulse of width $\tau=N\Delta t$, the weight W of the trajectory launched is given by the convolution of the pulse and Q

$$W=\frac{1}{\tau}\int_0^{\tau}dt\ Q(M\Delta t-t)\approx\frac{1}{N}\sum_{j=1}^{N}Q_j, \tag{9}$$

where the second equality is obtained by discretizing the time steps and noting that a trajectory which is never resonant ($j=0$) has no statistical weight. Substituting Eq. (8) into Eq. (9) gives

$$\begin{aligned}W&=\frac{1}{N}\sum_{j=1}^{N}\sum_{m=1}^{j}\mathscr{P}_m|a_f(m\Delta t)|^2\\&=\frac{1}{N}\sum_{m=1}^{N}(N-m+1)|a_f(m\Delta t)|^2\mathscr{P}_m.\end{aligned} \tag{10}$$

The equality in Eq. (10) follows from the number of terms in the inner sum, which depends explicitly on the index of the outer sum. This is the mathematical equivalent of noting that the overall statistical weight does not depend on the specific number of consecutive resonant configurations (the index j), but only on the number of ways of launching a trajectory from within one of the independent consecutive sequences (the index m). For the present argument, we make the assumption that $|\boldsymbol{\mu}_{fg}\cdot\mathbf{E}|^2$ is constant for all configurations which are on resonance (the Condon approximation). Then, we can substitute Eq. (7) into Eq. (10) to obtain the weighting of different trajectories for an excitation pulse of duration $\tau=N\Delta t$. We find

$$W\approx\frac{(\Delta t)^2}{4\hbar^2\tau}|\boldsymbol{\mu}_{fg}\cdot\mathbf{E}|^2\sum_{m=1}^{N}(N-m+1)m^2\prod_{n=1}^{m}P(n). \tag{11}$$

Figure 2 presents the statistical weight W as determined by Eq. (11) for different values of τ using the known joint probability distribution $P(n)$ (Fig. 1). As is intuitive from Fig. 1, it can be seen in Fig. 2 that W reaches its asymptotic value for pulse durations $\geqslant$20 fs. That is, for a sufficiently long excitation interaction, all trajectories chosen by random selection of resonant configurations should be given identical statistical weights independent of the number of consecutive configurations on resonance. This is a direct reflection of the rapid decay of the joint probability distribution $P(t)$. Nevertheless, for very short excitation pulses, this would not be valid.

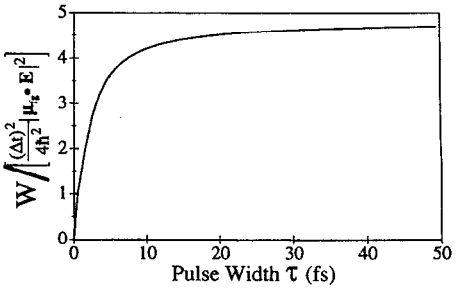

FIG. 2. Statistical weight for initiating an excited state trajectory as a function of excitation pulse duration, calculated from Eq. (11). See the text for details.

In all the work discussed below, we have convolved the calculated spectral transients with a 300 fs Gaussian. As the convolution samples starting configurations over a period significantly longer than the resonance correlation time, equal weights provide the correct ensemble average. Use of a 300 fs pulse allows us to make meaningful comparisons to the experiments[3,4] which have an instrument response on this time scale. Finally, the convolution smoothes out some of the noise inherent in the computation of spectra from only 20 trajectories.

III. ULTRAFAST PUMP–PROBE SPECTROSCOPY OF THE HYDRATED ELECTRON

The most critical test of any scientific model is how well it reproduces known experimental observables. Thus, before we use the microscopic information available from the molecular dynamics simulations of the hydrated electron to provide a detailed interpretation of the experimentally measured ultrafast spectroscopy, it is prudent to examine the strengths and shortcomings of this model in reproducing experimental results. Previous simulations[6] have been able to duplicate well the width, intensity, and general shape of the equilibrium absorption spectrum of the hydrated electron. The peak frequency, however, is calculated to be ~0.7 eV blueshifted from experiment. With a simple linear frequency shift that matches the computed and measured ground state absorption, there has been good general agreement between the ultrafast spectral dynamics computed via computer simulation[7–10] and those transients measured in electron photoinjection[1,2] and transient hole-burning[3–5] experiments.

Figure 3 displays a precise comparison between experimental ultrafast transients measured by Barbara and co-workers[21] and those computed with this Hamiltonian-based model of the hydrated electron. In making this comparison, we have simply shifted the frequencies of all computed transients by 0.62 eV, a value in accord[18] with the

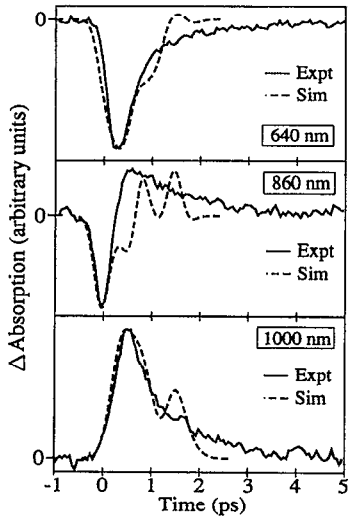

FIG. 3. Comparison of ultrafast spectroscopic transients measured in the laboratory (solid lines) and computed via molecular dynamics simulation (dashed lines) at three different wavelengths. The 640, 860, and 1000 nm traces correspond (Ref. 18) to simulated transients at 2.6, 2.2, and 2.0 eV, respectively. The transients are scaled to have the same maximum amplitude. Experimental data provided by Reid and Barbara (Ref. 21).

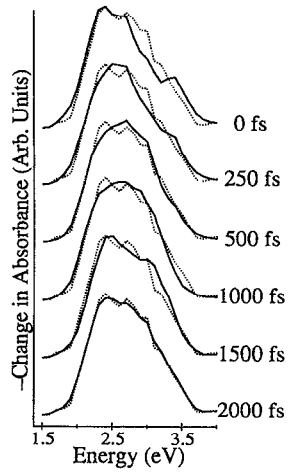

FIG. 4. Transient bleach dynamics for the hydrated electron at various time delays after photoexcitation (solid lines) referenced against the equilibrium absorption spectrum (dotted lines) for a pump energy of 2.27 eV.

difference observed between the simulated and experimental ground state absorption. As the experiment does not yield accurate absolute intensities, both sets of spectra were normalized to the same maximum amplitude, and since the $t=0$ point was not accurately determined in the experiments,[21] the absolute position in time of the 860 nm experimental transient was slightly adjusted (by ~100 fs) for better agreement. Except for these changes, there are no adjustable parameters. As can be seen in Fig. 3, the agreement is outstanding. The simulations reproduce the experimentally observed 1000 nm transient absorption, 640 nm transient bleach, and the initial bleach which overshoots into a net transient absorption at 860 nm with remarkable accuracy for delay time up to 1.5 ps.

What differences there are between the calculated and experimental transient spectra differ fall into two predominant categories. First, the simulated transients show oscillations which are not present on the experimental traces. These oscillations are the result of insufficient sampling over the phase of a low frequency intermolecular solvent mode coupled to the electronic dynamics, and are discussed in more detail in Sec. III D below. Second, while the simulated transients match the experimental ones well at early times, the simulated traces appear to decay roughly a factor of 2 faster at longer delays. The present description of the electron is expected to give an excited state lifetime which is too short due to the classical model used for solvent vibrations.[8] This is consistent with the excellent agreement at early times when the transient spectroscopy is dominated by solvation dynamics rather than the nonradiative lifetime.

Given the overall agreement between simulation and experiment, we can explain the observed ultrafast spectroscopy on the basis of the microscopic information available from the molecular dynamics simulations. In Secs. III A–III C, we present the individual transient bleach, absorption, and stimulated emission components and describe the underlying solvent motions that give rise to each. We then present the complete transient hole-burning spectroscopy of the hydrated electron, and show how each of the three components plays its part in the signals observed by experiment.

A. Transient bleach component

Figure 4 displays the calculated transient bleach spectra for the hydrated electron photoexcited at 2.27 eV (780 nm) at various time delays (solid curves). The calculated equilibrium absorption spectrum,[8] which would have been produced by uniform bleaching of the entire band, is shown normalized to equal area at each time delay (dotted curves) to emphasize the shape of the holes. Rapid solvent fluctuations cause the initial (pump–probe delay labeled $t=0$) hole to be quite broad, nearly the full width of the equilibrium absorption. The excitation pulse, which is tuned to the red side of the absorption spectrum, does cause some extra bleaching to the red and leaves a small bleach deficit on the blue side of the equilibrium spectrum, but the spectral hole is poorly resolved. By 250 fs, the hole has broadened somewhat and blueshifted and by 500 fs the hole shape is not distinguishable, within the noise, from the equilibrium absorption. This rapid washout of the initially bleached hole created on the red side of the spectrum is in agreement with previous adiabatic transient hole-burning calculations for the hydrated electron.[19]

For delays ≥ 1 ps, however, the calculated transient bleach spectra show continued evolution which contributes to the experimentally measurable total spectroscopy. Although the shape of the hole remains indistinct, the red edge of the transient bleach continues to blueshift past the red onset of the equilibrium absorption, leading to a slightly blueshifted spectrum at a delay of 1500 fs. While this shift looks small in comparison to the equilibrium absorption, it does lead to large net changes in absorption on the steeply rising and falling edges of the spectrum. This becomes espe-

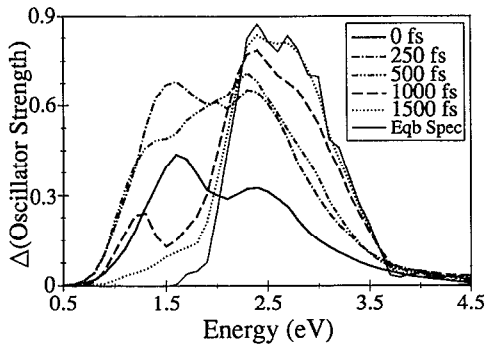

FIG. 5. Transient absorption spectral component for the hydrated electron at various time delays after photoexcitation in absolute intensity units, including contributions from both excited state electrons and electrons that have returned to the ground state. The thin solid line shows the equilibrium ground state absorption spectrum for reference.

cially apparent at the wavelengths immediately to the red of the excitation laser (1.9–2.3 eV). For example, the net absorption cross section at 2.1 eV decreases by a factor of 3 between 500 fs and 1.5 ps delay. This continuing blueshift on the ps time scale, which was missed in the earlier adiabatic simulations (which terminated calculation after 1 ps),[19] represents a significant portion of the observed complexity. In fact, these bleaching dynamics explain most of the net transient spectral dynamics observed between 500 and 750 nm.[10] By time delays of 2 ps and longer, the transient hole-burning spectrum is identical to the equilibrium absorption, and no further shifts or changes are observed.

This overall blueshift of the transient bleach must be a reflection of a portion of aqueous solvation dynamics which takes place on the picosecond time scale. Although it is not evident in the response functions presented in the preceding paper[11] due to the short excited state residence time of the hydrated electron, picosecond solvent relaxation of water has been observed in other simulations[22] and by experiment.[23] In previous work studying polarized spectroscopy of the hydrated electron, we found that while isotropic fluctuations coupled to the electron relaxed quickly, the relaxation of anisotropic fluctuations occurred on the picosecond time scale.[9] This is a consequence of the fact that memory of the original cavity orientation is maintained for times ≥ 1 ps, as is apparent in an earlier calculation of the transition dipole autocorrelation function.[19] This slow reorientation of the hydrated electron indicates that anisotropic solvent fluctuations take several picoseconds to completely randomize the initial subset of solvent configurations selected by the excitation laser. Thus, transient hole-burning dynamics make a nonnegligible contribution to the total spectroscopy of the hydrated electron even at relatively long time delays.

B. Excited state absorption component

The calculated excited state absorption contribution to the complete hole-burning spectroscopy of the hydrated electron is presented in absolute units in Fig. 5. These traces show the dynamic spectroscopy of the excited state trajectories as well as including spectral contributions from configurations in which the electron has nonadiabatically returned to the ground state. Thus, these spectra contain information about both the evolution of the excited state absorption spectrum and the re-establishment of the equilibrium spectrum after the radiationless decay. The large growth in overall spectral amplitude seen between the 0 and 250 fs traces is the result of the convolution with the 300 fs Gaussian instrument function; since the excited state absorption spectrum before excitation is zero by definition, the convolution leads to the observed delay in the establishment of the full spectral intensity. The thin solid curve in Fig. 5 marks the equilibrium ground state absorption spectrum for reference.

Initially, there has been very little nonadiabatic relaxation to the ground state, and the observed trace labeled $t=0$ is essentially the nascent excited state absorption spectrum. This characteristic spectrum peaks in the infrared, and is similar to that predicted in previous experimental[1,2] and theoretical[8] work. Since the ground state absorption is centered at roughly the same place as the blue feature of the excited state spectrum, nonadiabatic relaxation will lead to the apparent relative growth of this peak. Indeed, by 250 fs delay, the two features are now of nearly equal intensity, indicating substantial relaxation to the ground state. This trend continues through delays of 500 and 1000 fs, until by 1500 fs there is very little excited state contribution to the overall spectroscopy; at 1500 fs the spectrum closely resembles that of the equilibrium ground state.

Careful inspection of Fig. 5 reveals that the lower energy feature of the excited state spectrum undergoes a dynamic redshift over the course of the experiment. This peak, which starts out near 1.6 eV at $t=0$, has shifted to 1.4 eV by $t=500$ fs and can be seen at 1.2 eV at 1000 fs delay. At first glance, this phenomenon appears somewhat surprising given that the energy gap between the excited state and higher lying states is actually increasing during this period.[11] However, the absorption cross sections to the first two of these states on the red edge of this band undergo a significant increase with time, leading to the apparent redshift of the entire band. This is directly related to the microscopic changes induced by the solvation response. Immediately after photoexcitation, the nearly spherical cavity supports three orthogonally oriented p-like states; optical transitions between the lowest of these states and the upper two are symmetry forbidden. As the solvent responds to the electrical and mechanical perturbation of photoexcitation, the unoccupied upper two states become increasingly distorted, losing their resemblance to p states as solvent molecules enter the nodal region of the excited state electron. This distortion of the low-lying excited states, along with the accompanying changes in shape of the excited electron, lead to a solvation-induced net increase in oscillator strength for these two transitions, producing the observed redshift of the excited state spectrum in this region.

A slightly different effect occurs in the blue spectral tail of the excited state absorption spectrum. The solvation response produces a slight gradual increase in the energy of the higher lying continuum states following photoexcitation.[11] As the oscillator strength between the excited state electron and these highly delocalized states is relatively unaffected by

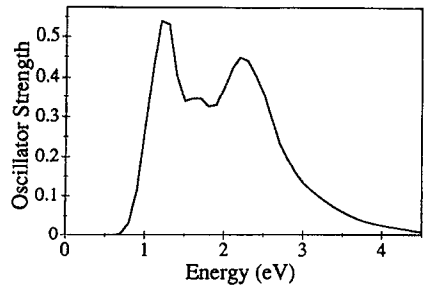

FIG. 6. Absorption spectrum of the equilibrated excited state of the hydrated electron in absolute intensity units, obtained from configurations in which the electron occupied the excited state for longer than 1 ps after photoexcitation.

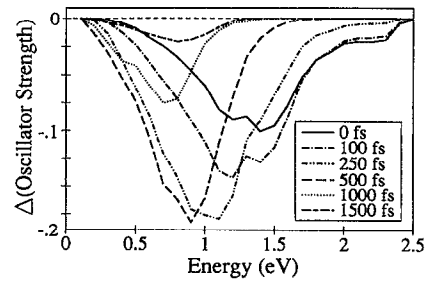

FIG. 7. Stimulated emission spectral component for the hydrated electron at various time delays after photoexcitation in absolute intensity units.

small changes in energy, the solvation response leads to a small blueshift of the excited state absorption spectral tail. The two competing processes, the increasing cross section of the lower energy states and the blueshifting of the higher lying continuum states leads to a complex evolution of the overall transient absorption spectrum. Both of these processes appear to relax with the 240 fs time scale of the solvent response,[11] and the absorption spectrum of those electrons which remain in the excited state does not appear to undergo further evolution beyond time delays of 1 ps. These complex spectral dynamics are responsible for much of the complicated behavior observed in the ultrafast transient hole-burning experiments.

Figure 6 presents the equilibrium excited state absorption spectrum of the hydrated electron, constructed from every third configuration in which the electron occupied the excited state for times ≥ 1 ps (~650 total configurations). This double-humped spectrum is qualitatively similar in appearance to the "equilibrium" excited state spectrum computed with the same model for electron injection,[8] but with two important differences. First, the entire spectrum of Fig. 6 is a few tenths of an eV blueshifted from that computed in the injection work. This is a consequence of the solvation dynamics which have increased the gap between the occupied excited state and higher states in the photoexcitation case but which are not yet complete in the photoinjection case.[11] Second, the splitting between the features in the excited state spectrum after electron injection is a little smaller than that seen in Fig. 6. This is also a direct repercussion of incomplete solvation dynamics in the injection case: the upper two p-like states have not distorted enough to increase their oscillator strength, and the continuum states have not undergone their solvation-induced blueshift. Thus, the same solvation dynamics which lead to a smaller energy gap between the ground and first excited states following photoinjection than following photoexcitation are also responsible for the observed differences in the transient spectroscopy.

The other important information contained in Fig. 5 concerns formation of the equilibrium ground state spectrum after nonadiabatic relaxation. The results of Fig. 5 suggest that the equilibrium spectrum simply grows in smoothly with time, and show little evidence for subsequent ground state spectral evolution. By 1500 fs, the transient spectrum is nearly identical to the equilibrium spectrum except for a little residual excited state absorption evident to the red of 2.0 eV. The equilibrium ground and excited state spectra have similar oscillator strengths near 2.3 eV, leading to the possibility of isosbestic behavior at this wavelength. Indeed, a quasi-isosbestic point (which becomes a true isosbestic point for time delays ≥ 1000 fs when the excited state spectrum ceases to evolve) is observed near 2.3 eV, indicating that the ground state equilibrium spectrum is formed virtually instantaneously within the instrumental resolution. This rapid re-establishment of the equilibrium spectrum upon nonadiabatic relaxation is in agreement with our earlier work,[10] as well as with the results of experiments and simulations studying spectral dynamics after photoinjection.[1,2,7,8] Note that the combination of rapid establishment of the ground state spectrum and the complex evolution of the excited state spectrum leads to the strong dynamic spectral blueshift in the 1.9–2.3 eV region which is responsible for much of the significant deviation from simple two-state kinetics.[10]

C. Stimulated emission component

The final contribution to the complete transient spectroscopy of the hydrated electron is due to stimulated emission, shown in absolute units in Fig. 7. The increase and decrease in emission intensity with time are the result of the instrumental resolution and the nonadiabatic return to the ground state, respectively. Since the electron has no internal structure and cannot undergo internal energy redistribution, the initial emission energy which occurs before the solvation response must be the same as the excitation energy (i.e., the $t=0$ Stokes' shift is zero). While there is evidence for a small peak at the excitation laser wavelength near 2.3 eV in the $t=0$ spectrum, the instrument function has already convoluted the 25 fs inertial response into the observed trace, leading to a large apparent initial Stokes' shift. This phenomenon, the inability to detect part of the initial Stokes' shift due to poor time resolution, has been discussed in the literature and a recipe has been provided for estimating the fraction of the missed response.[24] Still, once the rapid inertial dynamics are complete, the dynamic redshift of the emission spectrum provides a measure of the time-dependent energy gap, and hence, a direct route to the nonequilibrium solvent response function presented in the preceding paper.[11]

The subsequent evolution of the stimulated emission spectrum seen in Fig. 7 shows that the electron continues to

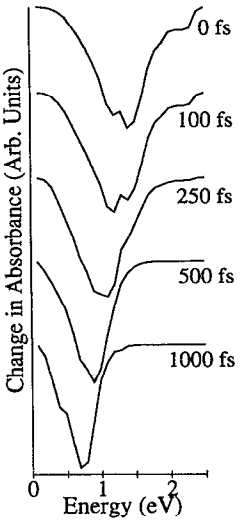

FIG. 8. Stimulated emission spectral component for the hydrated electron at various time delays after photoexcitation. Each trace has been scaled to the same maximum amplitude to clarify the dynamic changes in peak emission frequency and spectral width. The scaled spectra have been vertically offset for ease of comparison.

undergo its enormous Stokes' shift. The equilibrium emission spectrum ($t \geqslant 1000$ fs) peaks around 0.7 eV, indicating a relaxation of nearly 75% of the initial excitation energy, possibly the largest fractional Stokes' shift ever observed. Both the average and peak frequencies of the emission spectrum redshift with the 240 fs decay time constant of the solvent relaxation,[11] and little change in the shape or peak wavelength of the emission spectrum is observed after time delays of 1 ps. Within a few hundred femtoseconds, the large initial Stokes' shift takes this stimulated emission component out of the probe wavelength range of present ultrafast technology, so that stimulated emission dynamics have not played an important role in any of the observed hydrated electron ultrafast spectroscopy to date.

Since they have not yet been observed experimentally, the emission spectra presented in Fig. 7 provide another way to test this detailed description of the hydrated electron. Unfortunately, the very large Stokes' shift which makes the hydrated electron a sensitive probe of solvation dynamics also places the emission spectrum in the mid-to-far infrared, an experimentally inconvenient place to work. Efforts to collect the spontaneous infrared emission (note that fluorescence would be weighted by the ω^3 spectrum of the vacuum fluctuations inducing the spontaneous transition, significantly altering the peak wavelength and shape from the stimulated emission spectra presented in Fig. 7) will be hampered by the extremely small fluorescence quantum yield and the possibility of interfering IR absorption due to vibrational bands of the solvent. However, it is probable that the newly developed technique of infrared upconversion[25] could probe the stimulated emission dynamics in a region where the solvent does not absorb, providing an independent measure of the excited state residence time and possibly some information about the dynamic Stokes' shift.

In addition to the large Stokes' shift, evolution of the

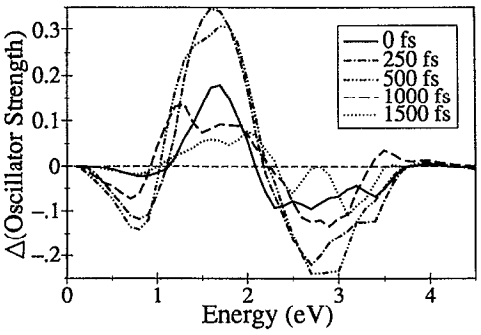

FIG. 9. Complete change in absorption for the hydrated electron at various time delays after photoexcitation in absolute intensity units. This result is the sum of those shown in Figs. 4, 5, and 7.

shape of the emission spectra also provides information about the underlying solvation response.[26] Figure 8 presents the time-dependent stimulated emission spectra normalized to equal maximum intensity and offset vertically for ease of comparison. Along with the rapid decay of emission at the pump frequency and the strong dynamic Stokes' shift, Fig. 8 also shows a dynamic narrowing of the overall emission spectrum. This narrowing is another consequence of the solvation dynamics coupled to the hydrated electron. At early times, the instrumental resolution convolutes emission from many different possible energy gaps, leading to a very broad stimulated emission spectrum. Once the solvation response is complete, emission occurs from the equilibrium excited state which has a relatively narrow distribution of energy gaps. The narrowing of the emission spectrum can also be explained by the effects of symmetry of the ground and excited electronic states. Immediately after excitation, solvent fluctuations affect the cylindrically symmetric occupied state in a somewhat different manner than the more spherically symmetric ground state, as evidenced by a strong initial change in the ground state energy. As the solvation response progresses, the ground state of the distorting cavity becomes more similar in shape to the occupied state, and solvent fluctuations change the energy of both states in a similar fashion. This can be seen in Fig. 4 of the preceding paper,[11] where at short times the ground state energy behaves quite differently from the excited state energy, but at longer times, the small energy oscillations caused by solvent interactions for the two states fluctuate nearly together, creating an energy difference which shows little overall change. Additional connections between the emission spectrum of the hydrated electron and aqueous solvation dynamics will be explored elsewhere.[27]

D. Complete transient spectroscopy

By combining the information presented in Figs. 4, 5, and 7, we can compute the total spectroscopic signal observed for transient hole burning of the hydrated electron. Figure 9 presents the complete spectral dynamics for the hydrated electron following photoexcitation at 2.27 eV (780 nm)[18] on the absolute intensity scale. The three underlying spectral components can all be observed in distinct spectral regions. The ground state bleaching dynamics dominates the

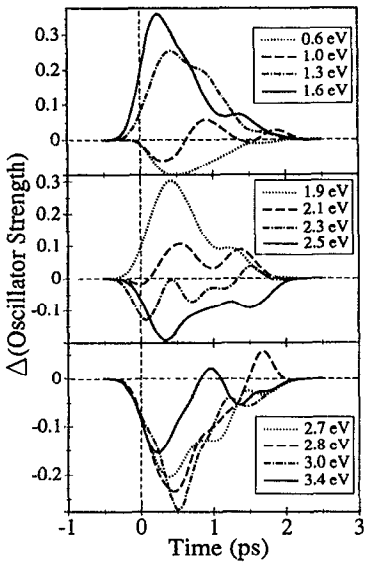

FIG. 10. Time domain spectral transients for the hydrated electron at various energies in absolute intensity units. See the text, Sec. III, for a discussion of the expected correspondence to experimental wavelengths.

portion of the spectral response to the blue of 2.5 eV. The strong excited state absorption is visible in the 1.5–2.0 eV region, and stimulated emission plays the dominant role to the red of 1.0 eV. As pointed out in our preliminary report,[10] these spectral dynamics cannot be described by a simple two-state kinetic model, as evidenced by complex spectral dynamics in the 2.0–2.5 eV (discussed earlier) and 0.8–1.3 eV spectral regions. An expanded view encompassing the 2–3 eV region, displayed on the wavelength scale of the transient hole-burning experiments,[4] was presented in Ref. 10.

The complicated spectral dynamics computed for the electron photoexcitation experiment (Fig. 9) can be explained by the effect of solvation dynamics on the spectral components comprising the overall signal. The strong spectral blueshift in the 2.0–2.5 eV region is a superposition of the slightly blueshifting excited state absorption on shorter time scales (Fig. 5) and the net blueshift of the ground state bleach on the ps time scale (Fig. 4). The dynamic redshift observed in the 0.8–1.3 eV region results from the large Stokes' shift of the stimulated emission (Fig. 7) combined with the redshift of the long-wavelength feature of the transient absorption (Fig. 5). Both these spectral regions show nonmonotonic (mixtures of net transient bleaching and net transient absorption) spectral dynamics, emphasizing the importance of solvation dynamics in the transient spectroscopy of the hydrated electron.

To further emphasize the complex spectral behavior following photoexcitation of the hydrated electron, we have computed time-domain spectral transients of the type measured directly in the laboratory, shown on the absolute intensity scale in Fig. 10. Noticeable in all the traces are oscillations on a ~300 fs time scale (frequencies around 100 cm^{-1}). These oscillations are most likely artifactual, resulting from insufficient sampling over the phase of intermolecular solvent modes which are strongly coupled to the electronic dynamics. As discussed in the preceding paper, the initial solvent response is dominated by phononlike translational motions of the solvent which take place at these frequencies, and correspond well with features observed in the Fourier transform of the solvent response function.[11] Ultrafast spectral transients computed using only 15 trajectories showed an enhancement of the oscillations compared to those presented in Fig. 10 which were averaged over all 20 trajectories. This indicates that these oscillations do damp out with increased sampling, and indeed reflect statistical error.

Despite this noise due to insufficient sampling, there is a great deal of information to be gained from the traces of Fig. 10. The center section shows some of the transient spectral dynamics for the experimentally accessible wavelength region. As discussed above (Fig. 3), these traces are in good agreement with experiment; even the small absolute amplitude of the computed 2.1 eV trace, for example, is consistent with the extra noise present in the measured ~900 nm experimental trace.[4] The upper section of Fig. 10 shows predicted spectral dynamics well into the infrared. The redshifting excited state spectrum (Fig. 5) leads to a slower absorption rise at longer wavelengths, as can be seen comparing the 1.6 and 1.3 eV traces. At 1.0 eV, stimulated emission dominates the spectral response until enough time has elapsed for the stronger excited state absorption to redshift to this wavelength, leading to nonmonotonic spectral dynamics. At 0.6 eV, the rise and decay of the stimulated emission is observed; as mentioned above, this feature might possibly be measurable by IR upconversion in regions where the solvent does not absorb. The lower portion of Fig. 10 shows the predicted blue and near-UV spectral responses. The bleach recovery rate increases slightly towards increasing energy, reflecting the overall blueshift of the transient hole. At the bluest wavelength presented, 3.4 eV, the cross section of the tail of the excited state absorption becomes comparable to that of the equilibrium spectrum, leading to a more rapid spectral recovery.

IV. CONCLUSIONS

In summary, we have used quantum nonadiabatic molecular dynamics simulations to understand the ultrafast transient hole-burning spectroscopy of the hydrated electron. The calculated spectral transients are in excellent agreement with experimental results, implying that the simulations accurately model the underlying solvation dynamics. While there is no distinct hole shape evident in the transient bleach, correlations in solvent fluctuations which decay on the picosecond time scale lead to bleaching dynamics which do play a role in the observed transient spectroscopy. The excited state absorption of the photoexcited hydrated electron shows a double-humped spectrum with a blue spectral tail; the long wavelength feature of this spectrum redshifts with solvation due to an increase in oscillator strength to the lowest lying higher excited states, while the tail of the spectrum undergoes a slight solvation-induced blueshift. Following nonadiabatic transition, the ground state equilibrium spectrum is established on a time scale fast compared to the instrumental

resolution. The stimulated emission from the excited aqueous electron is characterized by an enormous Stokes shift and an observed spectral width which narrows significantly with time. Both of these features of the emission dynamics are explained in terms of the solvent response. Each of these three spectral components plays a significant role in the ultrafast traces observed by experiment, making the solvated electron an outstanding theoretical and experimental probe of microscopic solvation dynamics.

ACKNOWLEDGMENTS

This work was supported by the National Science Foundation. One of the authors (B.J.S) gratefully acknowledges the support of NSF Postdoctoral Research Fellowship Grant No. CHE-9301479 awarded in 1993, and the allocation of computational resources from the San Diego Supercomputing Center.

[1] A. Migus, Y. Gauduel, J.-L. Martin, and A. Antonetti, Phys. Rev. Lett. **58**, 1559 (1987).
[2] F. H. Long, H. Lu, and K. B. Eisenthal, Phys. Rev. Lett. **64**, 1469 (1990).
[3] J. C. Alfano, P. K. Walhout, Y. Kimura, and P. F. Barbara, J. Chem. Phys. **98**, 5996 (1993).
[4] Y. Kimura, J. C. Alfano, P. K. Walhout, and P. F. Barbara, J. Phys. Chem. **98**, 3450 (1994).
[5] P. J. Reid, C. Silva, P. K. Walhout, and P. F. Barbara, Chem. Phys. Lett. (in press).
[6] J. Schnitker, K. Motakabbir, P. J. Rossky, and R. A. Friesner, Phys. Rev. Lett. **60**, 456 (1988).
[7] F. A. Webster, J. Schnitker, M. S. Friedrichs, R. A. Friesner, and P. J. Rossky, Phys. Rev. Lett. **66**, 3172 (1991).
[8] T. H. Murphrey and P. J. Rossky, J. Chem. Phys. **99**, 515 (1993).
[9] B. J. Schwartz and P. J. Rossky, Phys. Rev. Lett. **72**, 3282 (1994).
[10] B. J. Schwartz and P. J. Rossky, J. Phys. Chem. **98**, 4489 (1994).
[11] B. J. Schwartz and P. J. Rossky, J. Chem. Phys. **101**, 6902 (1994).
[12] E. Keszei, T. H. Murphrey, and P. J. Rossky, J. Phys. Chem. (submitted).
[13] E. Keszei, S. Nagy, T. H. Murphrey, and P. J. Rossky, J. Chem. Phys. **99**, 2004 (1993).
[14] F. A. Webster, P. J. Rossky, and R. A. Friesner, Comput. Phys. Commun. **63**, 494 (1991).
[15] F. Webster, E. T. Wang, P. J. Rossky, and R. A. Friesner, J. Chem. Phys. **100**, 4835 (1994).
[16] K. Toukan and A. Rahman, Phys. Rev. B **31**, 2643 (1985).
[17] J. Schnitker and P. J. Rossky, J. Chem. Phys. **86**, 3462 (1987).
[18] All figures presented in eV in this paper are wavelengths computed directly from the simulations. While a simple linear frequency shift of 0.67 eV was used for the pump wavelength and provides for an excellent match between the calculated and experimental ground state absorption, this shift clearly cannot be applied to the extreme spectral ranges (e.g., the stimulated emission which peaks near 0.7 eV). We have used a constant linear shift of 0.62 eV applied to the simulated transients for the comparison of Fig. 1, and expect that the general spectral trends and fractional magnitude of the Stokes shift will be in good agreement with experiment.
[19] K. A. Motakabbir, J. Schnitker, and P. J. Rossky, J. Chem. Phys. **90**, 6916 (1989).
[20] S. J. Rosenthal, B. J. Schwartz, and P. J. Rossky, Chem. Phys. Lett. (in press).
[21] P. J. Reid and P. F. Barbara (private communication).
[22] See, e.g., M. Maroncelli and G. R. Fleming, J. Chem. Phys. **89**, 5044 (1988).
[23] See, e.g., W. Jarzeba, G. C. Walker, A. E. Johnson, M. A. Kahlow, and P. F. Barbara, J. Phys. Chem. **92**, 7039 (1988).
[24] R. S. Fee and M. Maroncelli, Chem. Phys. **183**, 235 (1994).
[25] See, e.g., J. N. Moore, P. A. Hansen, and R. M. Hochstrasser, Chem. Phys. Lett. **138**, 110 (1987).
[26] M. Maroncelli, J. Mol. Liq. **57**, 1 (1993).
[27] B. J. Schwartz and P. J. Rossky (unpublished).